Fetuin B Is a Secreted Hepatocyte Factor Linking Steatosis to Impaired Glucose Metabolism

Resource

Cell Metabolism

Fetuin B Is a Secreted Hepatocyte Factor Linking Steatosis to Impaired Glucose Metabolism

Graphical Abstract

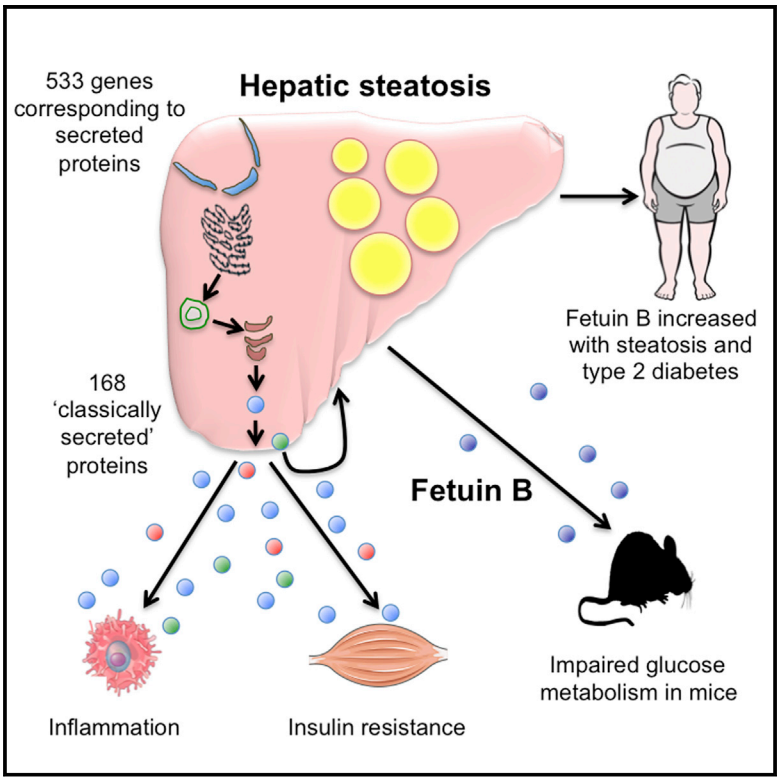

Authors

Ruth C. Meex, Andrew J. Hoy, Alexander Morris, ..., Graeme I. Lancaster, Clinton R. Bruce, Matthew J. Watt

Correspondence

matthew.watt@monash.edu

In Brief

Meex et al. use proteomic approaches to identify steatosis as a factor that changes protein secretion in hepatocytes. Secreted factors from steatotic hepatocytes caused insulin resistance and inflammation. One secreted protein, fetuin B, was identified as a hepatokine that is increased in type 2 diabetes and causes impaired glucose metabolism.

Highlights

- Factors released by steatotic hepatocytes cause insulin resistance and inflammation
- The complement of proteins secreted by hepatocytes is impacted by steatosis
- Fetuin B is secreted by hepatocytes and is increased in type 2 diabetes patients
- Fetuin B knockdown improves glucose metabolism in obese mice

Accession Numbers

GSE73726

Meex et al., 2015, Cell Metabolism 22, 1078–1089
December 1, 2015 ©2015 Elsevier Inc.
http://dx.doi.org/10.1016/j.cmet.2015.09.023

CellPress

Cell Metabolism
Resource

Fetuin B Is a Secreted Hepatocyte Factor Linking Steatosis to Impaired Glucose Metabolism

Ruth C. Meex,[1] Andrew J. Hoy,[1,9] Alexander Morris,[1] Russell D. Brown,[1] Jennifer C.Y. Lo,[1] Melissa Burke,[2,3] Robert J.A. Goode,[4] Bronwyn A. Kingwell,[5] Michael J. Kraakman,[5] Mark A. Febbraio,[5,6] Jan Willem Greve,[7] Sander S. Rensen,[7] Mark P. Molloy,[8] Graeme I. Lancaster,[5] Clinton R. Bruce,[1,10] and Matthew J. Watt[1,*]

[1]Monash Biomedicine Discovery Institute, Metabolic Disease and Obesity Program, and Biology of Lipid Metabolism Laboratory, Department of Physiology, Monash University, Clayton, VIC 3800, Australia
[2]Biotechnology Research Laboratories, Department of Physiology, Monash University, Clayton, VIC 3800, Australia
[3]Mill Hill Laboratory, The Francis Crick Institute, London NW7 1AA, UK
[4]Department of Biochemistry and Molecular Biology, Monash University, Clayton, VIC 3800, Australia
[5]Baker IDI Heart and Diabetes Institute, Melbourne, VIC 3004, Australia
[6]The Garvan Institute of Medical Research, Sydney, NSW 2010, Australia
[7]NUTRIM School of Nutrition and Translational Research in Metabolism, Maastricht University Medical Centre, Department of General Surgery, Maastricht, the Netherlands
[8]Australian Proteome Analysis Facility, Macquarie University, Sydney, NSW 2109, Australia
[9]Present address: Discipline of Physiology, School of Medical Sciences and Bosch Institute, University of Sydney, Sydney, NSW 2006, Australia
[10]Present address: Centre for Physical Activity and Nutrition Research, School of Exercise and Nutrition Science, Deakin University, Burwood, VIC 3125, Australia
*Correspondence: matthew.watt@monash.edu
http://dx.doi.org/10.1016/j.cmet.2015.09.023

SUMMARY

Liver steatosis is associated with the development of insulin resistance and the pathogenesis of type 2 diabetes. We tested the hypothesis that protein signals originating from steatotic hepatocytes communicate with other cells to modulate metabolic phenotypes. We show that the secreted factors from steatotic hepatocytes induce pro-inflammatory signaling and insulin resistance in cultured cells. Next, we identified 168 hepatokines, of which 32 were differentially secreted in steatotic versus non-steatotic hepatocytes. Targeted analysis showed that fetuin B was increased in humans with liver steatosis and patients with type 2 diabetes. Fetuin B impaired insulin action in myotubes and hepatocytes and caused glucose intolerance in mice. Silencing of fetuin B in obese mice improved glucose tolerance. We conclude that the protein secretory profile of hepatocytes is altered with steatosis and is linked to inflammation and insulin resistance. Therefore, preventing steatosis may limit the development of dysregulated glucose metabolism in settings of overnutrition.

INTRODUCTION

The liver plays a central role in systemic glucose and lipid metabolism. Accumulation of excess lipid in the liver, clinically known as hepatic steatosis, is an abnormality that characterizes obesity and type 2 diabetes. Steatosis develops largely as a consequence of caloric overload and is reversed rapidly upon consumption of a hypocaloric diet (Petersen et al., 2005). Steatosis is a component of non-alcoholic fatty liver disease (NAFLD) (Day and James, 1998), a serious medical condition affecting ~20%–40% of adults in the United States (Browning et al., 2004) and ~70% of morbidly obese individuals (Bellentani et al., 2000). NAFLD precedes the development of non-alcoholic steatohepatitis (NASH) and is closely linked with other metabolic disorders, including insulin resistance, type 2 diabetes, dyslipidemia, and cardiovascular disease (Chitturi et al., 2004). The factors linking these disorders remain unresolved.

Hepatic lipid content is regulated by a complex interplay between free fatty acid uptake and oxidation, uptake of fatty acids from chylomicron-derived triglycerides, triglyceride synthesis through fatty acid re-esterification and de novo lipogenesis, and triglyceride secretion contained within very-low-density lipoproteins (Samuel and Shulman, 2012). Therefore, defects within any of these processes can cause an imbalance between lipid supply and demand and, subsequently, drive hepatic steatosis. Hepatic steatosis in rodents develops rapidly in the setting of overnutrition (Kraegen et al., 1991; Stewart et al., 2009; Turner et al., 2013) and occurs at a time point that normally precedes the development of other abnormalities associated with caloric excess, including adipocyte hypertrophy and obesity development (Strissel et al., 2007), adipocyte death (Strissel et al., 2007), macrophage infiltration and inflammation of adipose tissue (Strissel et al., 2007; Turner et al., 2013; Xu et al., 2003), skeletal muscle lipid accumulation, insulin resistance (Kraegen et al., 1991; Turner et al., 2013), and whole-body hyperglycemia and hyperinsulinemia (Turner et al., 2013; Xu et al., 2003). Targeted studies have identified several liver-derived endocrine factors that impact the peripheral metabolism, including fetuin A (Pal et al., 2012), adropin (Kumar et al., 2008), angiopoietin-like protein 6 (Angptl6) (Oike et al., 2005), fibroblast growth factor 21 (FGF21) (Kharitonenkov et al., 2005), and selenoprotein P (Misu

et al., 2010), demonstrating that factors secreted from hepatocytes or hepatokines are involved in metabolic cross-talk. Furthermore, cDNA microarray and proteomic studies have reported changes in intracellular gene expression and protein content of whole liver with caloric overload in rodents and humans (Kirpich et al., 2011; Toye et al., 2007; Younossi et al., 2005; Zhang et al., 2010). Collectively, these observations are consistent with the notion that liver steatosis is an early manifestation in the etiology of metabolic dysfunction associated with caloric (fatty acid) overload and that protein signals originating from the steatotic liver may "cross-talk" with other tissues to influence metabolic and inflammatory function and, thereby, modulate metabolic phenotypes.

The aim of this study was to test whether hepatic steatosis, independent of inflammation, alters the hepatocyte protein secretory profile and to test whether changes in the secretory products contribute to the development of metabolic dysfunction in other cell types. We show that liver steatosis alters the hepatokine secretion profile and produces a milieu that induces inflammation and insulin resistance in macrophages and skeletal muscle. Using discovery-based "omics" platforms, we identify fetuin-B as a liver-secreted protein that is elevated in patients with liver steatosis and type 2 diabetes and causes glucose intolerance in mice.

RESULTS

Short-Term High-Fat Feeding of C57Bl6/J Mice Causes Hepatic Steatosis and Glucose Intolerance but Not Inflammation or Liver Damage

The liver is composed of many cell types, including hepatocytes, stellate cells, endothelial cells, and numerous immune cell types. To identify hepatocyte-specific factors that are induced by steatosis, we developed an ex vivo model in which hepatocytes were isolated from mice that had been fed either standard chow or high-fat diet (HFD) for 6 weeks. At the time of hepatocyte isolation, mice fed a HFD exhibited increased body mass, increased epididymal fat mass, and glucose intolerance compared with chow-fed mice (Figures S1A–S1C). Plasma alanine aminotransferase (ALT) and aspartate aminotransferase (AST) levels were unaffected by high-fat feeding, demonstrating that the diet did not cause liver damage (Figure S1D).

Isolated Hepatocytes from High-Fat-Fed Mice Are Steatotic in the Absence of Inflammation

The purity of the hepatocyte isolation was first confirmed by flow cytometry and immunofluorescent staining. Incubation of the isolated cells with a fluorescein isothiocyanate (FITC)-conjugated anti-albumin antibody resulted in a shift in fluorescence intensity of the entire cell population (Figure 1A), demonstrating a highly pure hepatocyte population. There was no evidence of endothelial cells ($CD31^+$) in the isolated cell population, and macrophages/Kupffer cells ($CD45^+$ $F4/80^+$ cells) made up just 2.3% of the cell population (Figure 1B). Hepatocytes isolated from HFD-fed mice were fat-laden, as demonstrated by large and abundant intracellular lipid droplets (Figure 1C) and increased intracellular triacylglycerol content (Figure 1D). Steatosis can be accompanied by inflammation in vivo. However, there was no indication of proinflammatory serine/threonine kinase activation, as demonstrated by analysis of c-Jun terminal kinase (JNK) phosphorylation (indicating activity) and by a lack of nuclear factor of κ light polypeptide gene enhancer in B cells inhibitor α (IκBα) degradation (indicating activation of necrosis factor κB [NF-κB] signaling) (Figure 1E). These data establish a model in which hepatocytes are steatotic but are neither inflamed nor damaged, as occurs in NASH, and allow us to next determine the effect of simple steatosis on the hepatocyte secretome.

Secreted Products from Steatotic Hepatocytes Regulate Inflammation and Insulin Action in Other Cell Types: Evidence of Metabolic Cross-Talk

The induction of liver steatosis is associated with obesity-related disorders such as insulin resistance, inflammation, and dysregulated lipid metabolism (Abdul-Ghani et al., 2008; Kraegen et al., 1991; Larson-Meyer et al., 2011; Wicklow et al., 2012). In an attempt to model this pathophysiology in vitro, cultured myotubes and macrophages were incubated for 24 hr in the conditioned medium (CM) produced by hepatocytes from chow- and HFD-fed mice. Cells were then washed prior to functional assays to evaluate the metabolic and inflammatory responses of cells to the hepatocyte-secreted products.

Skeletal muscle is a major site for fatty acid metabolism and insulin-stimulated glucose disposal. Glucose uptake in L6 GLUT4myc myotubes was not different between chow and HFD CM in the basal (unstimulated) state. Insulin increased glucose uptake by 110% in myotubes exposed to chow CM and by only 53% in myotubes exposed to HFD CM (Figure 1F), demonstrating impaired insulin action. Short-term (2-h) exposure to HFD CM did not impair insulin action (data not shown), suggesting that HFD CM did not directly impair insulin signaling but instead affected other processes that impact insulin action. We reasoned that the decline in insulin action was associated with alterations in fatty acid metabolism, given the close association between these processes (Turner et al., 2013). Indeed, myotubes incubated in HFD CM showed small but significant increases in fatty acid uptake (12%), oxidation (10%), and triglyceride storage rates (14%) (Figure 1G), although we did not observe changes in diglyceride storage rates (Figure 1G).

Low-grade inflammation is often associated with HFD-induced insulin resistance. Incubation of macrophages with chow CM did not affect inflammatory signaling compared with untreated cells (data not shown). HFD CM induced a pro-inflammatory response, as demonstrated by increased phosphorylation of JNK and IκB kinase (IKK) (Figure 1H). Interestingly, pre-incubation of macrophages in HFD CM also exacerbated lipopolysaccharide (LPS)-induced inflammation (Figure 1H). Together, these experiments indicate that steatotic hepatocytes secrete products that induce selective components of pro-inflammatory pathways in macrophages and cause insulin resistance in skeletal muscle.

Steatosis Regulates the Protein Secretome in Hepatocytes

Having determined that steatotic hepatocytes secrete factors that influence the function of other cells, we next attempted to identify hepatocyte-derived secretory proteins involved in steatosis-induced metabolic dysregulation. A major challenge in

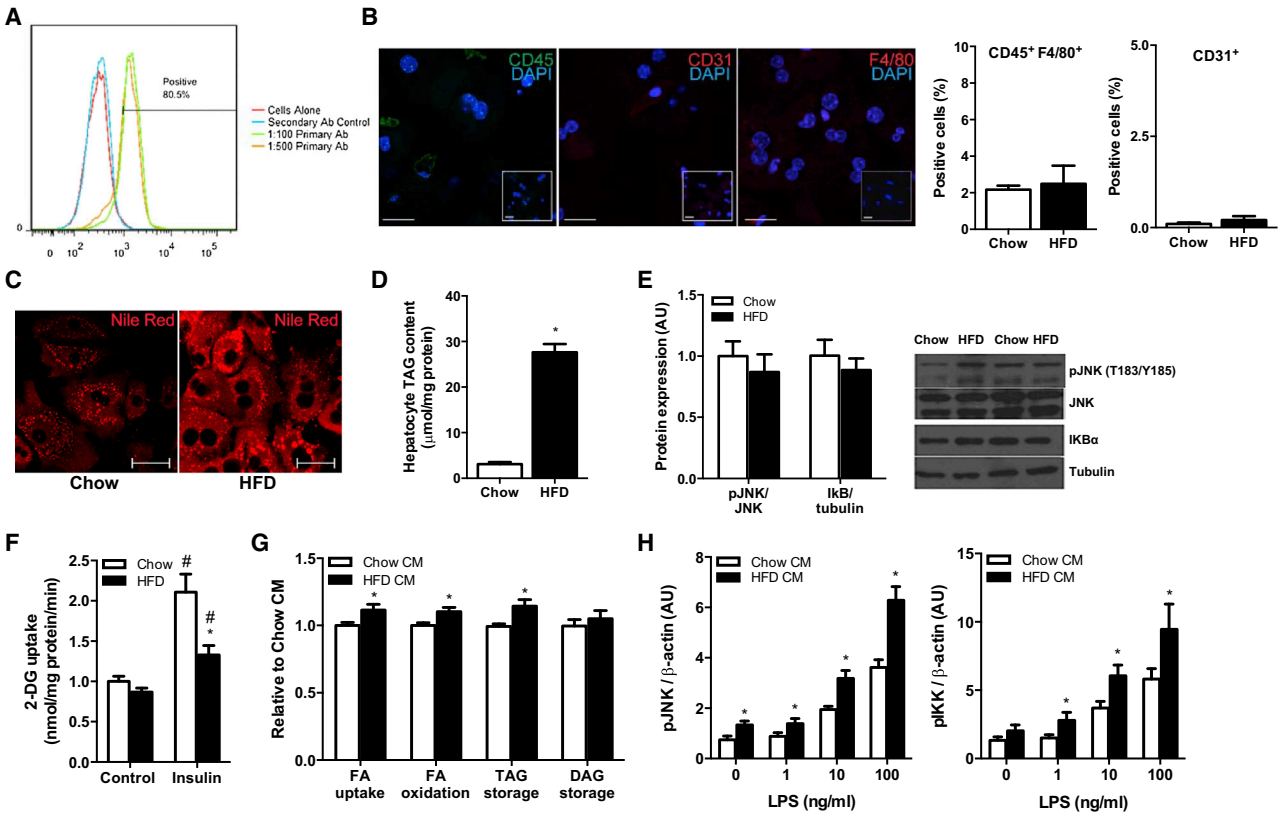

Figure 1. Steatotic Hepatocytes Secrete Factors that Cause Insulin Resistance and Promote Pro-inflammatory Signaling

(A–E) C57Bl/6J mice were fed a chow or HFD for 6 weeks. Hepatocytes were isolated, and the secreted products were collected.

(A) Purity of the hepatocyte isolation as shown by fluorescence-activated cell sorting analysis using a FITC-conjugated anti-albumin antibody.

(B) Immunofluorescence immunohistochemistry for CD45 (leukocytes), CD31 (endothelial cells), and F4/80 (macrophages) in cultured isolated hepatocytes. Inset, no primary antibody negative control. Quantification of cells positive for CD45 and F4/80 (macrophages) and CD31 is shown at the right. Isolated cells were cultured for 24 hr and trypsinized before flow cytometry (n = 3 independent donor mice). Scale bars, 25 μm.

(C) Nile Red staining showing increased neutral lipid accumulation in hepatocytes isolated from chow- versus HFD-fed mice. Scale bars, 50 μm (n = 1 biological replicate).

(D) Biochemical determination of triglyceride (TAG) content in cultured hepatocytes (n = 8 biological replicates per group). *p < 0.05 versus chow.

(E) Pro-inflammatory signaling in hepatocytes was similar between both groups, as measured by phosphorylation of JNK and expression of IκBα (n = 3 biological replicates, each containing 4 technical replicates/group). AU, arbitrary unit.

(F–H) L6-GLUT4myc myotubes or bone marrow-derived macrophages were incubated for 16 hr in CM collected from the isolated hepatocytes of chow- or HFD-fed mice.

(F) 2-deoxyglucose (2-DG) uptake in L6-GLUT4myc myotubes without (Control) or with 1 nM insulin (n = 3 biological replicates, each containing 3-4 technical replicates/group). *p < 0.05 versus chow CM, #p < 0.05 versus control within the same treatment.

(G) Fatty acid (FA) metabolism in L6-GLUT4myc myotubes (n = 3 biological replicates, each containing 10 technical replicates/group). *p < 0.05 versus chow CM.

(H) Bone marrow-derived macrophages (BMDMs) pre-treated in CM were incubated in LPS at the indicated concentrations for 30 min. Left: pJNK/β-actin. Right: pIKK/β-actin. n = 3 biological replicates, each performed with 3 technical replicates. *p < 0.05 versus chow CM.

All data are mean ± SEM.

assessing the hepatocyte secretome is delineating the contribution of hepatocytes from other cell types that reside in the liver. To overcome this limitation, we utilized the cell-based model of purified hepatocytes described above (Figures 1A and 1B). A second challenge associated with this model is determining the contribution of cytosolic contamination to the secretory profile. Cell death (trypan blue staining) was not different between hepatocytes exposed to collection medium for 0 or 24 hr or between hepatocytes derived from chow- or HFD-fed mice (Figure S2A). In support of this finding, lactate dehydrogenase levels in the culture medium were not different between chow and HFD hepatocytes (Figure S2C). The major non-muscle cytoskeletal actin, β-actin, was not detected in the cell culture medium by immunoblot (0, 8, and 24 hr; Figure S2B), and 39 of the 50 most abundant proteins detected in the culture medium are known secreted proteins (Table S1). Therefore, although cell death is inevitable, this was negligible, and the release of intracellular proteins into the "collection medium" was not different between treatment groups.

We cross-referenced the sequence of proteins detected in the conditioned medium with algorithms to predict classically secreted proteins that harbor an N-terminal signal sequence. Proteins that were detected in the culture medium without an N-terminal signal sequence could be secreted by non-classical

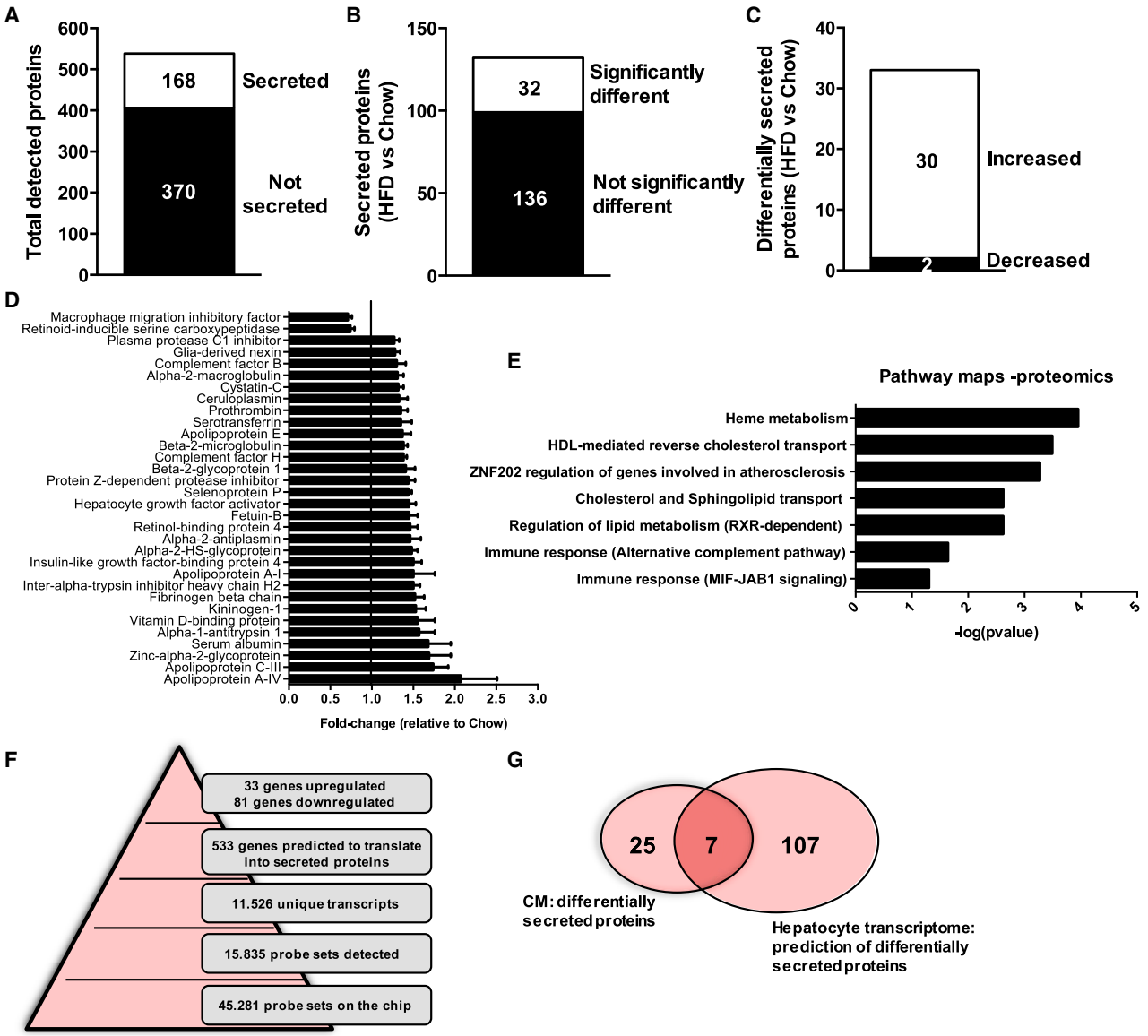

Figure 2. The Hepatocyte Protein Secretome Is Altered with Steatosis

(A) Proteins detected in the hepatocyte conditioned medium of chow and HFD hepatocytes. Secreted proteins are considered those with a N-terminal signal sequence or annotated as secreted in UniProt (keywords: GOCC or subcellular location) (n = 8 biological replicates performed in 2 independent analytical experiments).

(B) Secreted proteins that are significantly different between chow and HFD conditioned medium (n = 8 biological replicates performed in 2 independent experiments).

(C) Direction of change of proteins that are differentially secreted (n = 8 biological replicates performed in 2 independent experiments).

(D) List of differentially secreted proteins in chow and HFD conditioned medium.

(E) Enrichment analysis highlighting the top biological processes represented in the protein secretome of HFD CM. Enrichment analysis was performed against mouse proteins defined as secreted in the UniProt database.

(F) Representation of the cDNA microarray analysis from chow and HFD hepatocytes.

(G) Overlap of the differentially secreted proteins (from iTRAQ) and the predicted differentially secreted proteins using transcriptomics. Only seven genes/proteins were detected and changed in the same direction using both approaches (n = 8 biological replicates/group).

secretion mechanisms. However, for the purpose of these experiments, they were treated as "non-secreted" unless expressly annotated as secreted in UniProt.

Isobaric tags for relative and absolute quantitation (iTRAQ)-based proteomic analysis identified and quantitated 538 proteins, 370 which were designated non-secreted and 168 as secreted (Figure 2A). The secreted and non-secreted proteins are listed in Table S2. Of the secreted proteins, 136 (81%) exhibited no change in abundance between chow and HFD hepatocytes (Figure 2B), whereas 30 proteins were increased and two

were decreased in HFD compared with Chow CM (Figure 2C). A list of the differentially secreted proteins is presented in Figure 2D. Metacore was used to identify biological pathways associated with hepatocyte protein secretion differences mediated by steatosis. Enrichment analysis revealed an overrepresentation of secreted proteins associated with heme metabolism, cholesterol and sphingolipid transport, lipid metabolism, and immune response (Figure 2E). These processes are consistent with the important role of the liver in regulating metabolism and immune function.

Transcriptomic Approaches Do Not Accurately Predict the Hepatocyte Protein Secretion Profile

We also performed global transcriptomic analysis of hepatocytes in parallel with the protein secretion studies with the aim of determining whether the protein secretome could be predicted by changes in transcript levels. In total, there were 45,281 probe sets on the chip, and 15,835 probe sets were detected (Table S2), which corresponded to 11,526 unique transcripts. Of those unique transcripts, 533 genes were predicted to translate into secreted proteins based on bioinformatics profiling as described above. Of the genes corresponding to secreted proteins, 418 (78%) exhibited no change in abundance between chow and HFD hepatocytes, whereas 33 genes were upregulated by a HFD and 81 were downregulated (Figure 2F). To interpret these changes in a biological context, we analyzed the differentially secreted genes using Metacore and identified a significant, biologically relevant association of these genes with the immune response and insulin growth factor 1 (IGF-1) signaling. Therefore, aside from the immune response, the bioinformatics approach did not predict enrichment of similar biological pathways when comparing the secreted protein or transcriptome dataset. Consistent with this notion, the protein secretome was not predicted by changes in transcript levels (Figure 2G) with only seven transcripts/proteins identified as upregulated in both analyses. These are apolipoprotein A, zinc-α-2-glycoprotein, inter-α-trypsin inhibitor heavy chain H2, insulin-like growth factor-binding protein 4, α-2-HS-glycoprotein, α-2-antiplasmin, and hepatocyte growth factor activator. Therefore, consistent with previous comparative analyses of the murine transcriptome and proteome (Ghazalpour et al., 2011), these data demonstrate that the protein secretome cannot be accurately predicted by assessing changes in the transcriptome obtained from the same biological source, highlighting the fact that post-transcriptional events significantly affect the protein secretion profile in hepatocytes.

Fetuin B Is Increased in Obese Humans with Liver Steatosis

We next examined steatosis-regulated proteins for their involvement in glucose metabolism. Of the differentially secreted proteins, fetuin B was increased 1.5-fold in HFD compared with Chow hepatocytes based on iTRAQ mass spectrometry (Figure 2D). This was confirmed by independent immunoblot experiments of the secreted culture medium (Figure 3A, inset) and coincided with a 3-fold increase in hepatocyte fetuin B content (Figure 3B). Fetuin-B shares 22% homology with fetuin A, a circulating glycoprotein that causes insulin resistance by activating Toll-like receptors and inducing inflammatory signaling (Pal et al., 2012; Stefan and Häring, 2013a), and fetuin B levels have previously been associated with rodent obesity (Choi et al., 2010). Accordingly, we examined plasma and liver fetuin B levels in obese humans without or with steatotic livers (steatosis/NAFLD), as determined from liver biopsies. The participants' characteristics are included in Table 1. Plasma fetuin B levels were increased in obese participants with simple steatosis compared with obese participants without steatosis (Figure 3C). Liver fetuin B protein content was not different between groups (Figure S3A–S3C). Plasma fetuin B correlated positively with fasting insulin (Figure S3D) and homeostatic model assessment for insulin resistance (HOMA-IR), an index of insulin resistance (Figure 3D) and did not correlate with BMI (adiposity), the liver damage marker alanine aminotransferase, the inflammatory marker C-reactive protein, or blood lipids, including total cholesterol, high-density lipoprotein (HDL) cholesterol, low-density lipoprotein (LDL) cholesterol, triglycerides, and free fatty acids (Figures S3E–S3L).

Fetuin B Impairs Insulin Sensitivity in Myotubes and Hepatocytes

Examination of fetuin B in a second human cohort showed that plasma fetuin B levels were not increased in obese individuals without diabetes but increased in type 2 diabetes patients compared with lean, insulin-sensitive individuals (Figure 3E). This prompted us to examine the direct effect of fetuin B on glucose metabolism. Fetuin B decreased insulin-stimulated glucose uptake in myotubes (Figure 3F) in a time- and dose-dependent manner. Defects in insulin action only became evident after 24 hr of fetuin B treatment (no effects at 30 min or 2 hr, data not shown) and at fetuin B concentrations reported in human plasma (~300 μmol/l; Figures S3M–S3O; Denecke et al., 2003). Fetuin B also impaired insulin action in primary hepatocytes, as demonstrated by impaired insulin-mediated suppression of the gluconeogenic genes *G6pc* (encoding glucose-6-phosphatase) and *Pck1* (encoding cytosolic phosphoenolpyruvate carboxykinase) (Figures 3G and 3H), and tended to decrease ($p = 0.06$) insulin-mediated Akt phosphorylation (Figure 3I).

Fetuin B shares 22% homology with fetuin A, a circulating glycoprotein that causes insulin resistance by activating Toll-like receptors and inducing inflammatory signaling (Pal et al., 2012; Stefan and Häring, 2013a). Accordingly, we determined whether fetuin B could exert similar effects. Fetuin B treatment had no effect on pro-inflammatory signaling (Figure 3J) or cytokine release (Figure 3K) from primary bone marrow-derived macrophages, which contrasted the actions of the canonical TLR4 ligand LPS. Pro-inflammatory signaling was similarly unaffected in myotubes, as evidenced by similar phosphorylation of JNK ($p = 0.69$) and extracellular regulated kinase (ERK) ($p = 0.65$) and by similar contents of IκBα ($p = 0.43$) (Figure S4A–S4C). Consistent with these effects, plasma tumor necrosis factor α (TNF-α) levels were not increased 2 hr after fetuin B administration into lean mice (Figure 3L). Therefore, unlike fetuin A, physiological concentrations of fetuin B do not induce pro-inflammatory signaling.

Fetuin B Causes Glucose Intolerance but Not Insulin Resistance in Mice

To study the effects of fetuin B on glucose metabolism in vivo, recombinant fetuin B was injected intraperitoneally into mice,

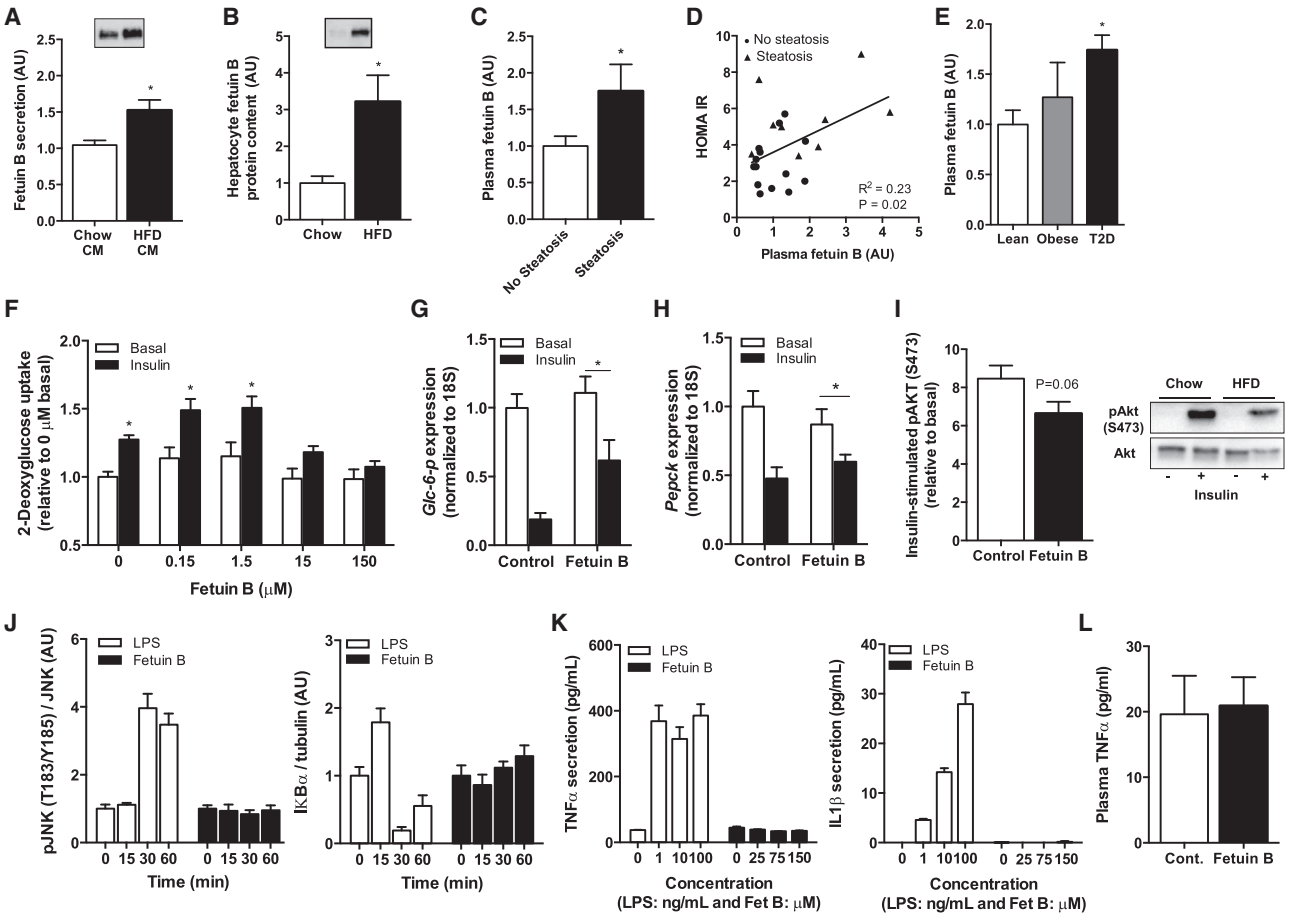

Figure 3. Fetuin B Is Upregulated in Individuals with Steatosis and Type 2 Diabetes and Causes Insulin Resistance but Not Inflammation in Cultured Cells

(A) Secreted fetuin B determined by immunoblot in the conditioned medium (n = 4/group from independent donor mice). *p < 0.05 versus chow CM. A representative immunoblot of fetuin B in the conditioned medium is shown above (left, chow CM; right, HFD CM). Equal loading was confirmed by imaging the stain-free gel.

(B) Fetuin B protein expression in isolated hepatocytes (n = 6/group obtained from independent donor mice). *p < 0.05 versus chow. A representative immunoblot is shown above (left, chow; right, HFD). The blot was normalized to total protein loading for each sample, which was obtained by visualization and quantification of the stain-free blot image.

(C) Plasma fetuin B levels in obese humans without (No Steatosis, n = 14) or with liver steatosis (Steatosis, n = 11). *p < 0.05 versus No Steatosis.

(D) Correlation between plasma fetuin B and HOMA-IR (n = 21).

(E) Plasma fetuin B levels in individuals who were lean insulin-sensitive (n = 9), obese insulin-sensitive (n = 5), or obese with type 2 diabetes (n = 14). *p < 0.05 versus Lean.

(F) 2-Deoxyglucose uptake in L6-GLUT4myc myotubes exposed to various concentrations of fetuin B for 24 hr. (n = 5/group from 2 independent experiments). *p < 0.05 versus basal at the same fetuin B concentration.

(G and H) *Glc-6-p* (G) and *Pepck* (H) expression in primary murine hepatocytes treated with fetuin B. Hepatocytes were incubated without (basal) or with 1 nM insulin for 2 hr before RNA extraction (n = 3 biological replicates, each performed with 3-4 technical replicates). *p < 0.05, main treatment effect (fetuin B).

(I) Phosphorylated Akt(Ser-473) during insulin stimulation (1 nM) in primary murine hepatocytes. A representative immunoblot is shown at the right (n = 3 biological replicates, each performed with 4 technical replicates).

(J) BMDMs were treated with 150 μM fetuin B or 100 ng/ml LPS at the indicated time points. Phosphorylated JNK (Thr-183/Tyr-185)/JNK and IκBα/tubulin content was determined by immunoblot (n = 3/condition from 1 experiment).

(K) BMDMs were treated with either LPS or fetuin B for 24 hr at the indicated concentrations. TNF-α and interleukin 1β (IL-1β) concentrations in the culture media were assessed by ELISA (n = 3/condition from 1 experiment).

(L) Mice were injected with recombinant fetuin B or control (Cont) 2 hs prior to glucose administration (2 g/kg) (n = 5/group). Plasma TNF-α was measured 15 min after glucose administration.

All data are mean ± SEM.

and glucose tolerance was assessed 2 hr later. Plasma fetuin B levels were increased 2 hr after fetuin B injection (Figure 4A). Glucose tolerance was impaired significantly in mice treated with fetuin B (Figure 4B), whereas plasma insulin levels were similar in fetuin B and control mice 15 min after glucose administration (Figure 4C). Fetuin B administration did not affect

Table 1. Participant Characteristics

	No Steatosis (n = 14)	Steatosis + IR (n = 11)	p Value
Age (years)	42.1 ± 2.4	37.9 ± 2.5	0.24
BMI (kg/m^2)	41.0 ± 1.8	46.5 ± 2.2	0.07
Glucose (mmol/l)	5.4 ± 0.2	5.4 ± 0.1	0.79
Insulin (pmol/l)	12.4 ± 1.4	22.6 ± 2.6	0.001[a]
HOMA-IR	3.0 ± 0.4	5.4 ± 0.6	0.002[a]
HbA1C (%)	5.9 ± 0.1	5.8 ± 0.1	0.56
Type 2 diabetes	None	None	
Total cholesterol (mmol/l)	4.7 ± 0.2	5.3 ± 0.4	0.12
HDL cholesterol (mmol/l)	1.1 ± 0.1	1.0 ± 0.1	0.28
Total/HDL cholesterol	4.1 ± 0.3	5.7 ± 0.5	0.001[a]
LDL cholesterol (mmol/l)	2.7 ± 0.2	3.6 ± 0.3	0.03[a]
Triglycerides (mmol/l)	1.8 ± 0.2	1.7 ± 0.3	0.9
Free fatty acids (mmol/l)	0.5 ± 0.1	0.6 ± 0.1	0.7
ALT (U/l)	19.9 ± 1.4	24.4 ± 3.5	0.19
AST (U/l)	16.2 ± 2.3	19.3 ± 1.8	0.35
hsCRP (mg/l)	10.1 ± 2.3	15.0 ± 5.2	0.36
Urea (mmol/l)	4.1 ± 0.2	3.4 ± 0.4	0.12
Creatinine (μmol/l)	77.8 ± 4.2	70.1 ± 2.0	0.16
Steatosis (grade 0–3)	0.0 ± 0.0	1.5 ± 0.2	0.001[a]
NASH	None	None	
Fibrosis (grade 0–3)	grade 0: n = 14	grade 0: n = 10	
		grade 1: n = 1	
Lobular inflammation (grade 0–2)	grade 0: n = 14	grade 0: n = 7	
		grade 1: n = 2	
		grade 2: n = 2	
Ballooning (grade 0–2)	grade 0: n = 14	grade 0: n = 8	
		grade 1: n = 3	
		grade 2: n = 0	
NAFLD activity score	0.0 ± 0.0	2.4 ± 0.4	

Data are expressed as mean ± SE.
[a]Significantly different from healthy controls.

insulin- or AMP-activated protein kinase (AMPK) signaling in the liver (Figure 4D) or skeletal muscle (data not shown) during the glucose tolerance test.

Insulin-mediated effects account for ~50% of glucose clearance during a glucose tolerance test (Ahrén and Pacini, 2002; Alonso et al., 2012; Best et al., 1996). Accordingly, we directly assessed insulin sensitivity by performing hyperinsulinemic-euglycemic clamping in mice 2 hr after intraperitoneal (i.p.) fetuin B administration. Mice were clamped at 10.7 ± 0.2 mmol/l glucose, and steady-state glucose levels were achieved in both groups. The glucose infusion rate required to maintain euglycemia was similar in both groups (Figure 4E), indicating equivalent whole-body insulin sensitivity. Neither the suppression of hepatic glucose output (Figure 4F) nor the glucose rate of disappearance (Figure 4G) was different between treatment groups. Independent experiments examining insulin sensitivity during a short-term intravenous insulin tolerance test also showed no effect of fetuin B on whole-body or tissue-specific insulin action (Figures S4D–S4F). Therefore, fetuin B did not affect hepatic or peripheral insulin sensitivity.

Glucose effectiveness refers to the capacity for glucose to enhance peripheral glucose uptake and suppress endogenous glucose production independent of insulin, and it accounts for the remaining ~50% of glucose clearance during a glucose tolerance test (Alonso et al., 2012; Best et al., 1996). Circulating plasma lactate levels increase in response to a glucose challenge because of a combination of tissue glucose uptake and glycolysis to form lactate, which is then released into the circulation. Decreased lactate production in the absence of any difference in insulin sensitivity has been linked to decreased glucose effectiveness (Best et al., 1996). Plasma lactate during a glucose challenge was decreased in mice pre-treated with fetuin B, suggestive of decreased glucose effectiveness in these mice (Figure 4H).

Reducing Fetuin B Improves Glucose Tolerance in Obese Mice

To confirm the effect of fetuin B on glucose metabolism in an independent experimental model, mice fed a high-fat diet for 6 weeks were injected with an adeno-associated virus (serotype 8) containing a short hairpin RNA (shRNA) against either fetuin B or a scrambled shRNA. Fetuin B shRNA decreased fetuin B expression in liver and plasma fetuin B by 33% and 72% compared with scramble shRNA (Figures 4I and 4J). The silencing effects were not restricted to the liver, with decreased fetuin B in white adipose tissue and hearts of fetuin B shRNA-treated mice (Figures S4G and S4H). The decrease in liver fetuin B was closely associated with changes in plasma fetuin B, supporting the premise that the liver is most likely a primary source of circulating fetuin B (Figure 4K). Body mass was not impacted by fetuin B shRNA (Figure 4L), whereas glucose tolerance was improved markedly in mice treated with fetuin B shRNA compared with littermates treated with control shRNA (Figure 4M). Collectively, these data demonstrate improved whole-body glucose metabolism upon reduction of circulating fetuin B in obese mice.

DISCUSSION

Hepatic steatosis is a common condition that is closely associated with obesity and type 2 diabetes. Clinical studies demonstrate that steatosis is more closely related to the development of insulin resistance than obesity per se (Fabbrini et al., 2009; Korenblat et al., 2008; Koska et al., 2008; Linder et al., 2014), indicating that signals originating from the steatotic liver might negatively affect insulin action via inter-tissue communication. We report that the hepatocyte protein secretion profile is altered by steatosis and that the combination of the hepatocyte secreted products causes insulin resistance and inflammation. We used this omics platform to identify proteins whose secretion is upregulated by steatosis and focused on fetuin B, a highly expressed liver protein that has been reported previously to be upregulated in obese mice. We also provide evidence that fetuin B is a hepatokine that is regulated by steatosis in humans, is

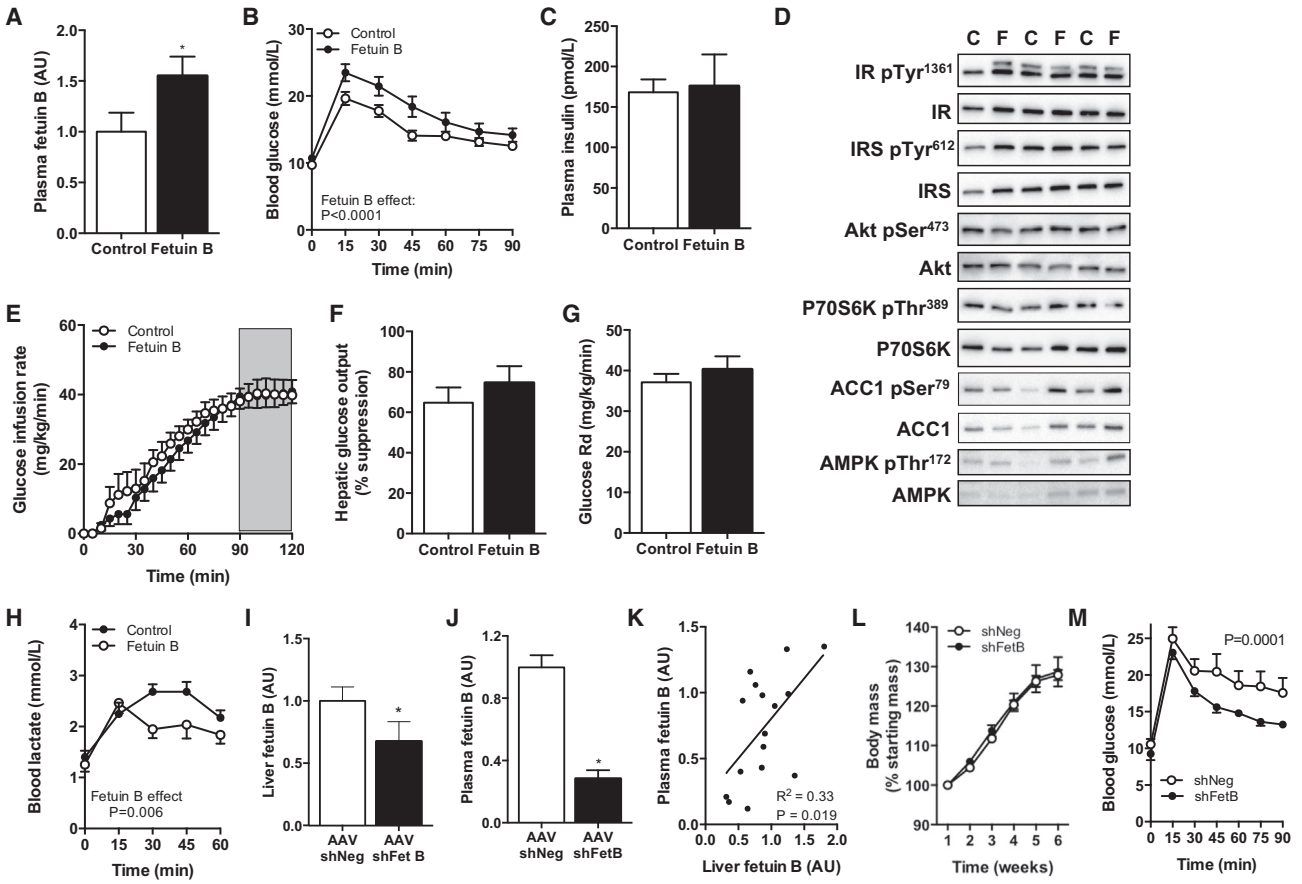

Figure 4. Fetuin B Causes Glucose Intolerance in Mice

(A) Plasma fetuin B levels in mice 2 hr after injection of recombinant fetuin B or control (n = 4/group). *p < 0.05 versus control.

(B) Glucose tolerance test (2 g/kg) in C57Bl/6J mice treated without or with fetuin B 2 hr prior to testing (n = 7 control, n = 8 fetuin B). p < 0.0001, main effect for fetuin B.

(C) Plasma insulin at 15 min of the glucose tolerance test (n = 4 per group).

(D) Insulin and AMPK signaling were unaffected by fetuin B administration during the glucose tolerance test. Mice were injected with fetuin B (F) or control (C) 2 hs prior to glucose administration. Tissues were freeze-clamped 15 min after glucose administration (2 g/kg). IR, insulin receptor; IRS, insulin receptor substrate; ACC, acetyl CoA carboxylase. Shown are representative blots of n = 8/group.

(E–G) Mice were injected i.p. with fetuin B 2 hr prior to hyperinsulinemic-euglycemic clamping.

(E) Glucose infusion rate (GIR) during clamping. The steady-state GIR is denoted by gray shading.

(F) Suppression of hepatic glucose output by insulin.

(G) Insulin-stimulated whole-body glucose rate of disappearance (Rd) (n = 7 control, n = 8 fetuin B).

(H) Plasma lactate during the glucose tolerance test (2 g/kg) (n = 5/group).

(I–M) C57Bl/6J mice were fed a high-fat diet for 6 weeks and treated with adeno-associated virus (AAV) containing a shRNA fetuin B or scramble shRNA for 5 weeks prior to experiments.

(I and J) Liver fetuin B content (I) and plasma fetuin B levels (J) in mice.

(K) Correlation between liver fetuin B and plasma fetuin B.

(L) Body mass of mice before and after AAV administration.

(M) Glucose tolerance tests in mice (2 mg/kg).

For all experiments, (n = 10 control, n = 6 fetuin B). *p < 0.05 versus shNeg.

All data are mean ± SEM.

elevated in type 2 diabetes, and causes glucose intolerance by modulating insulin-independent glucose metabolism.

Mapping of the murine liver identified ~7,000 proteins, of which 25% were also detected in the plasma (Lai et al., 2008), suggesting that the liver secretes many proteins to regulate systemic biological processes. The present studies have assessed the hepatocyte protein secretome and provide several important insights, supporting further mechanistic studies. First, we identified 538 proteins in the hepatocyte secretion medium, with 168 assigned as classically secreted, confirming the hepatocyte as a major producer of plasma proteins. In comparison, adipocytes secrete ~160 proteins (Crowe et al., 2009), and, given the involvement of adipokines in regulating metabolic phenotypes, these results implicate hepatokines as important regulators of biological processes. In addition, because two-thirds of the proteins identified in the conditioned medium do not contain a signal

peptide, it is likely that significant protein secretion from the hepatocyte occurs through unconventional secretory processes. In unconventional secretion, proteins that lack an N-terminal signal peptide are not delivered to the lumen of the ER but can be transported into the extracellular milieu via diverse pathways. These include transit across the plasma membrane independent of a cell surface transporter, secretory lysosome-mediated membrane fusion, plasma membrane budding, transport via exosomes produced in multivesicular bodies, secretory autophagy, and release via mitochondrial derived vesicles (Zhang and Schekman, 2013). Although the existence of unconventional secretion is widely accepted, targeted studies are required to delineate whether and how specific proteins identified in our studies are secreted from hepatocytes.

Next, we showed that diet-induced steatosis alters the hepatic protein secretion profile. The liver transcriptome and proteome are altered in mice fed a high-fat diet (Kirpich et al., 2011; Schmid et al., 2004) and in humans with steatosis (Greco et al., 2008; Younossi et al., 2005), and active protein synthesis in the ER is reduced in the livers of obese mice (Fu et al., 2012). These latter findings indicate altered protein secretion because the ER/Golgi-dependent secretory pathway exports the vast majority of secreted proteins. We extend these observations in reporting that the hepatocyte secretome is sensitive to steatosis, with altered secretion in 20% of the classically secreted proteins. Bioinformatic analyses of the overall changes in protein secretion predicted alterations in inflammation and metabolism, and cell-based studies confirmed that the secretome from the steatotic hepatocyte impaired insulin action in muscle and hepatocytes and activated pro-inflammatory pathways in macrophages. It is noteworthy that more than half of the differentially secreted proteins in our studies are upregulated in the serum of type 2 diabetes patients (Kaur et al., 2012), suggesting that dysregulated hepatic protein secretion induced by steatosis might be an important component of diabetes development and that a subset of the protein secretome we identified as steatosis-responsive might predict diabetes development. Further work will be needed to delineate whether and how these proteins, either individually or in combination, contribute to the development of insulin resistance and other metabolic dysfunctions.

The utility of the proteomics approach is evidenced by the identification of fetuin B as a steatosis-responsive hepatokine that negatively affects glucose metabolism. Fetuin B is a member of the cystatin superfamily of cysteine protease inhibitors and shares 22% homology with fetuin A (Denecke et al., 2003). Fetuin A (also known as α-2-HS-glycoprotein) is increased in patients with steatosis (Stefan et al., 2006). Its circulating levels are correlated negatively with insulin sensitivity in humans (Mori et al., 2006), and insulin signaling is improved in *Ahsg*$^{-/-}$ (encoding fetuin A) mice (Mathews et al., 2002). Fetuin A induces metabolic dysfunction through a number of mechanisms that include inhibition of insulin receptor tyrosine kinase activity and the promotion of inflammation in immune cells and adipocytes (Stefan and Häring, 2013b). Recently, fetuin A has been identified as an adaptor protein for saturated fatty acid-induced activation of Toll-like receptor 4 signaling, which promoted lipid-induced insulin resistance (Pal et al., 2012), and the fetuin A/free fatty acid (FFA) interaction appears to predict the development of insulin resistance in humans (Stefan and Häring, 2013a). Importantly, we show in this study that fetuin B acts in a manner quite distinct from that of fetuin A.

Previous studies have reported increased fetuin-B levels in obese rodents (Choi et al., 2010). However, the role of fetuin B in metabolic regulation and the clinical relevance of these observations were unknown. We report that fetuin B is increased in the plasma of type 2 diabetes patients and individuals with hepatic steatosis and that plasma fetuin B levels are associated positively with insulin resistance. Fetuin B decreased insulin sensitivity in cultured muscle and hepatocytes when administered at physiological concentrations and did not activate proinflammatory signaling. In contrast, although fetuin B caused glucose intolerance in mice, it did not impair insulin signaling after glucose administration and did not reduce insulin sensitivity during hyperinsulinemic-euglycemic clamping in mice. Although the findings in these different models appear somewhat discordant, they are not without explanation. Insulin resistance in humans develops over many years, and the clamp studies in mice were conducted 2 hr after fetuin B administration. Furthermore, the cell culture studies demonstrated that fetuin B effects on insulin action are both dose- and time-dependent (i.e., insulin resistance was evident after 24 hr but not after 2 h), and we surmise that the relatively small (yet physiological) and transient (2 h) increase in i.p.-delivered fetuin B might have been insufficient to impair insulin action in mice in vivo.

Glucose disposal is controlled by the combined effects of insulin secretion, insulin sensitivity of peripheral tissues, and glucose effectiveness, which refers to the ability of glucose to promote its own disposal, independently of insulin (Alonso et al., 2012; Best et al., 1996). Glucose effectiveness is at least as important as insulin for glucose clearance, accounting for ~50% of an oral glucose tolerance test in normal individuals and ~80% in obese, insulin-resistant individuals (Best et al., 1996). Similar contributions have been reported for lean and obese mice (Alonso et al., 2012). Although glucose effectiveness has been presumed to occur by the mass action of glucose to drive glucose into cells in a gradient-dependent manner, it is now clear that this process is regulated. For example, glucose effectiveness is suppressed by ~50% in non-obese men with impaired glucose tolerance and type 2 diabetes patients (Best et al., 1996), and glucose effectiveness can be enhanced by exercise training in humans (Nishida et al., 2001) and in mice by FGF19 acting through the CNS (Morton et al., 2013). Although a large body of physiological and clinical data has described the existence and regulation of glucose effectiveness, the underlying cellular and molecular processes are currently unknown. In the liver, glucoregulatory hormones such as glucagon and cortisol impair glucose effectiveness, as do chronically elevated FFA levels (Tonelli et al., 2005). Although peripheral glucose effectiveness (e.g., muscle) is the dominant component of whole-body glucose effectiveness (Mevorach et al., 1998), its molecular regulation is largely unknown (Tonelli et al., 2005).

Our in vivo studies in mice demonstrate that fetuin B causes glucose intolerance in lean mice, independent of changes in plasma insulin and insulin signal transduction during glucose administration or changes in insulin sensitivity during clamping. Rather, our studies suggest that glucose effectiveness is reduced by fetuin B. In support of this conclusion, fetuin B reduced plasma lactate levels during a glucose challenge, which

is consistent with previous studies reporting reduced glycolysis of glucose to lactate and impaired glucose effectiveness in *ob/ob* mice (Morton et al., 2013). Although we do not know the mechanism of action for fetuin B, we can conclude that fetuin B does not impact several putative regulators of glucose effectiveness or insulin action, including proinflammatory signaling (Figures 3J and 3K), adipocyte lipolysis (Figures S4I and S4J), fatty acid metabolism in myotubes (Figure S4K) and hepatocytes (Figure S4L), or AMPK signaling in skeletal muscle and liver (Figure S4M). Despite this limitation, the data establish a model whereby fetuin B secretion from the liver is increased by steatosis and diminishes glucose lowering through insulin-independent mechanisms. Furthermore, partial silencing of fetuin B improved glucose tolerance in obese mice, independent of weight loss, suggesting a role for fetuin B in the pathogenesis of diabetes.

In conclusion, these data provide a comprehensive examination of the hepatocyte protein secretome and demonstrate marked changes in response to simple steatosis, a metabolic abnormality that is common in type 2 diabetes and dyslipidemia. Conceptually, our work extends our understanding of the pathogenesis of diabetes by demonstrating that the combined secreted products from the steatotic hepatocyte are proinflammatory and promote insulin resistance. The identification of fetuin B as a steatosis-responsive hepatokine that induces dysregulated glucose metabolism demonstrates the utility of this approach and paves the way for validating other molecules that could be important in the pathogenesis of diabetes and cardiovascular disease.

EXPERIMENTAL PROCEDURES

Additional procedures can be found in the Supplemental Experimental Procedures.

Human Studies

Human studies were approved by the Medical Ethical Committee of Maastricht University and the Alfred Hospital Human Research Ethics Committee. All participants provided written informed consent before participation in the studies. In one cohort, a fasted plasma sample was obtained before surgery, and a liver biopsy was taken during surgery to assess the presence of liver steatosis according to the Brunt classification (Brunt et al., 1999). The healthy group (n = 14) comprised patients with <5% steatotic hepatocytes (score 0). The steatotic group (n = 11) comprised patients with >5% steatotic hepatocytes (score 1–3) without significant inflammation, as observed after H&E staining (i.e., no intra-acinar inflammatory foci per 20 fields with a 20 ocular and no portal tract inflammation). In the second cohort, venous blood samples were obtained from an antecubital vein after an overnight fasting in 28 males who were lean insulin-sensitive (n = 9), obese insulin-sensitive (n = 5), and obese with type 2 diabetes (n = 14). Detailed study protocols are outlined in the Supplemental Experimental Procedures.

Animal Studies

Animal studies were approved by the Monash University School of Biomedical Science Animal Ethics Committee. Male C57BL/6 mice aged 8 weeks were fed either a chow (4.6% fat) or high fat diet (36% fat) for 6 weeks prior to hepatocyte isolation, which was performed as described in the Supplemental Experimental Procedures. Mice were fasted for 4 hr from 07:00 hr and then injected i.p. with fetuin B (1 μg/g body mass) (Life Research) 2 hr prior to glucose tolerance tests (2 g/kg D-glucose), insulin tolerance tests (1 U/kg), or hyperinsulinemic-euglycemic clamping (4 mU/kg/min) as described previously (Borg et al., 2014; Mason et al., 2014). In separate experiments, mice were fed a HFD for 6 weeks. After 1 week, an adeno-associated virus, serotype 8 (AAV8), driven by a cytomegalovirus (CMV) promoter (1×10^{12} genome copy [gc]) containing an shRNA sequence specific for murine fetuin B (Vector Laboratories, shADV-259329) was injected via the tail vein. Control mice were injected with the same vector containing LacZ.

Cell Culture

Cell culture was performed in L6 GLUT4myc myotubes, primary murine hepatocytes, and bone marrow-derived macrophages. Primary hepatocytes were obtained from anesthetized (3% isoflurane) mice by inserting a 24-gauge catheter into the hepatic portal vein and perfusing with Hank's buffered salt solution and collagenase buffer (Liberase research-grade, 50 μg/ml, Roche) in series. Conditioned medium was collected in EX-CELL 325 protein-free Chinese hamster ovary (CHO) serum-free medium (SAFC Biosciences) for 24 hr and then placed on cells for 16 hr prior to functional analyses. Fetuin B was purchased from Life Research. Detailed protocols of functional assays are outlined in the Supplemental Experimental Procedures.

iTRAQ Sample Preparation and Data Acquisition

In short, proteins were reduced with tris(2-carboxyethyl)phosphine (TCEP), alkylated with methyl methanethiosulfonate (MMTS), digested with trypsin, and labeled with iTRAQ 8-plex reagents following the manufacturer's instructions. The iTRAQ-labeled samples were combined in equal ratios, fractionated using strong cation exchange (SCX), and analyzed by reverse-phase nanoLC electrospray ionization (ESI) MS/MS using a top ten data-dependent acquisition strategy with a 5600 TripleTOF mass spectrometer. See Supplemental Experimental Procedures for detailed procedures.

The mass spectrometry proteomics data have been deposited into the ProteomeXchange Consortium [1] via the PRIDE partner repository with the dataset identifier PXD002858.

Flow Cytometry

Cells were analyzed using LSR II (BD Biosciences), and data analysis was completed using the Flowjo cytometric analysis program (version 10).

Transcriptomics

Mouse-amplified RNA quality was ascertained on an Agilent Bioanalyzer 2100 using the NanoChip protocol. 750 ng of amplified RNA was hybridized to the Illumina MouseWG-6 v2 Expression BeadChip. The chip was washed and then coupled with Cy3 and scanned in the Illumina iScan reader. Genes with an expression difference of $\geq$1.20-fold with a 95% confidence interval between conditions were considered to be different.

All biochemical measures, blood chemistry, immunoblotting, qRT-PCR, and immunohistochemistry were performed by standard approaches and are detailed in the Supplemental Experimental Procedures.

Statistical Analysis

Statistical analysis was performed using paired or unpaired Student's t tests, one- or two-way ANOVA, or repeated measures ANOVA where appropriate. Individual means were compared using a Bonferroni post hoc analysis when required. Statistical significance was set a priori at $p \leq 0.05$. Data are reported as mean ± SEM.

ACCESSION NUMBERS

The accession number for the whole-genome expression profiling reported in this paper is Gene Expression Omnibus: GSE73726.

SUPPLEMENTAL INFORMATION

Supplemental Information includes Supplemental Experimental Procedures, four figures, and two tables and can be found with this article online at http://dx.doi.org/10.1016/j.cmet.2015.09.023.

AUTHOR CONTRIBUTIONS

Conceptualization, R.C.M., A.J.H., and M.J.W.; Investigation, R.C.M., A.M., R.B., S.S.R., J.W.G., J.C.Y.L., G.I.L., M.J.K., M.M., C.R.B., and M.J.W.; Data

Analysis, R.C.M., A.J.H., A.M., M.B., J.C.Y.L., R.J.A.G., M.J.K., G.I.L., and M.J.W.; Writing – Original Draft, R.C.R. and M.J.W.; Writing – Review & Editing, A.J.H., A.M., M.B., J.C.Y.L., R.J.A.G., B.A.K., M.J.K., M.A.F., S.S.R., M.M., G.I.L., and C.R.B.

ACKNOWLEDGMENTS

We acknowledge the technical assistance of Xiaomin Song, Dana Pascovici, and Thiri Zaw (Australian Proteome Analysis Facility) and Michael de Veer (Monash University). This work was supported by research grants from the National Health and Medical Research Council of Australia (ID 1061278), Diabetes Australia Research Trust (to M.J.W.), and Monash University (to M.J.W.) and fellowships from the National Health and Medical Research Council of Australia (to A.J.H., ID 606766; to M.A.F., ID APP1021168, to B.A.K., ID 1059454; and to M.J.W., IDs 606460 and 1077703).

Received: April 21, 2015
Revised: August 4, 2015
Accepted: September 23, 2015
Published: October 22, 2015

REFERENCES

Abdul-Ghani, M.A., Matsuda, M., and DeFronzo, R.A. (2008). Strong association between insulin resistance in liver and skeletal muscle in non-diabetic subjects. Diabet. Med. *25*, 1289–1294.

Ahrén, B., and Pacini, G. (2002). Insufficient islet compensation to insulin resistance vs. reduced glucose effectiveness in glucose-intolerant mice. Am. J. Physiol. Endocrinol. Metab. *283*, E738–E744.

Alonso, L.C., Watanabe, Y., Stefanovski, D., Lee, E.J., Singamsetty, S., Romano, L.C., Zou, B., Garcia-Ocaña, A., Bergman, R.N., and O'Donnell, C.P. (2012). Simultaneous measurement of insulin sensitivity, insulin secretion, and the disposition index in conscious unhandled mice. Obesity (Silver Spring) *20*, 1403–1412.

Bellentani, S., Saccoccio, G., Masutti, F., Crocè, L.S., Brandi, G., Sasso, F., Cristanini, G., and Tiribelli, C. (2000). Prevalence of and risk factors for hepatic steatosis in Northern Italy. Ann. Intern. Med. *132*, 112–117.

Best, J.D., Kahn, S.E., Ader, M., Watanabe, R.M., Ni, T.C., and Bergman, R.N. (1996). Role of glucose effectiveness in the determination of glucose tolerance. Diabetes Care *19*, 1018–1030.

Borg, M.L., Lemus, M., Reichenbach, A., Selathurai, A., Oldfield, B.J., Andrews, Z.B., and Watt, M.J. (2014). Hypothalamic neurogenesis is not required for the improved insulin sensitivity following exercise training. Diabetes *63*, 3647–3658.

Browning, J.D., Szczepaniak, L.S., Dobbins, R., Nuremberg, P., Horton, J.D., Cohen, J.C., Grundy, S.M., and Hobbs, H.H. (2004). Prevalence of hepatic steatosis in an urban population in the United States: impact of ethnicity. Hepatology *40*, 1387–1395.

Brunt, E.M., Janney, C.G., Di Bisceglie, A.M., Neuschwander-Tetri, B.A., and Bacon, B.R. (1999). Nonalcoholic steatohepatitis: a proposal for grading and staging the histological lesions. Am. J. Gastroenterol. *94*, 2467–2474.

Chitturi, S., Farrell, G.C., and George, J. (2004). Non-alcoholic steatohepatitis in the Asia-Pacific region: future shock? J. Gastroenterol. Hepatol. *19*, 368–374.

Choi, J.W., Wang, X., Joo, J.I., Kim, D.H., Oh, T.S., Choi, D.K., and Yun, J.W. (2010). Plasma proteome analysis in diet-induced obesity-prone and obesity-resistant rats. Proteomics *10*, 4386–4400.

Crowe, S., Wu, L.E., Economou, C., Turpin, S.M., Matzaris, M., Hoehn, K.L., Hevener, A.L., James, D.E., Duh, E.J., and Watt, M.J. (2009). Pigment epithelium-derived factor contributes to insulin resistance in obesity. Cell Metab. *10*, 40–47.

Day, C.P., and James, O.F. (1998). Steatohepatitis: a tale of two "hits"? Gastroenterology *114*, 842–845.

Denecke, B., Gräber, S., Schäfer, C., Heiss, A., Wöltje, M., and Jahnen-Dechent, W. (2003). Tissue distribution and activity testing suggest a similar but not identical function of fetuin-B and fetuin-A. Biochem. J. *376*, 135–145.

Fabbrini, E., Magkos, F., Mohammed, B.S., Pietka, T., Abumrad, N.A., Patterson, B.W., Okunade, A., and Klein, S. (2009). Intrahepatic fat, not visceral fat, is linked with metabolic complications of obesity. Proc. Natl. Acad. Sci. USA *106*, 15430–15435.

Fu, S., Fan, J., Blanco, J., Gimenez-Cassina, A., Danial, N.N., Watkins, S.M., and Hotamisligil, G.S. (2012). Polysome profiling in liver identifies dynamic regulation of endoplasmic reticulum translatome by obesity and fasting. PLoS Genet. *8*, e1002902.

Ghazalpour, A., Bennett, B., Petyuk, V.A., Orozco, L., Hagopian, R., Mungrue, I.N., Farber, C.R., Sinsheimer, J., Kang, H.M., Furlotte, N., et al. (2011). Comparative analysis of proteome and transcriptome variation in mouse. PLoS Genet. *7*, e1001393.

Greco, D., Kotronen, A., Westerbacka, J., Puig, O., Arkkila, P., Kiviluoto, T., Laitinen, S., Kolak, M., Fisher, R.M., Hamsten, A., et al. (2008). Gene expression in human NAFLD. Am. J. Physiol. Gastrointest. Liver Physiol. *294*, G1281–G1287.

Kaur, P., Rizk, N.M., Ibrahim, S., Younes, N., Uppal, A., Dennis, K., Karve, T., Blakeslee, K., Kwagyan, J., Zirie, M., et al. (2012). iTRAQ-based quantitative protein expression profiling and MRM verification of markers in type 2 diabetes. J. Proteome Res. *11*, 5527–5539.

Kharitonenkov, A., Shiyanova, T.L., Koester, A., Ford, A.M., Micanovic, R., Galbreath, E.J., Sandusky, G.E., Hammond, L.J., Moyers, J.S., Owens, R.A., et al. (2005). FGF-21 as a novel metabolic regulator. J. Clin. Invest. *115*, 1627–1635.

Kirpich, I.A., Gobejishvili, L.N., Homme, M.B., Waigel, S., Cave, M., Arteel, G., Barve, S.S., McClain, C.J., and Deaciuc, I.V. (2011). Integrated hepatic transcriptome and proteome analysis of mice with high-fat diet-induced nonalcoholic fatty liver disease. J. Nutr. Biochem. *22*, 38–45.

Korenblat, K.M., Fabbrini, E., Mohammed, B.S., and Klein, S. (2008). Liver, muscle, and adipose tissue insulin action is directly related to intrahepatic triglyceride content in obese subjects. Gastroenterology *134*, 1369–1375.

Koska, J., Stefan, N., Permana, P.A., Weyer, C., Sonoda, M., Bogardus, C., Smith, S.R., Joanisse, D.R., Funahashi, T., Krakoff, J., and Bunt, J.C. (2008). Increased fat accumulation in liver may link insulin resistance with subcutaneous abdominal adipocyte enlargement, visceral adiposity, and hypoadiponectinemia in obese individuals. Am. J. Clin. Nutr. *87*, 295–302.

Kraegen, E.W., Clark, P.W., Jenkins, A.B., Daley, E.A., Chisholm, D.J., and Storlien, L.H. (1991). Development of muscle insulin resistance after liver insulin resistance in high-fat-fed rats. Diabetes *40*, 1397–1403.

Kumar, K.G., Trevaskis, J.L., Lam, D.D., Sutton, G.M., Koza, R.A., Chouljenko, V.N., Kousoulas, K.G., Rogers, P.M., Kesterson, R.A., Thearle, M., et al. (2008). Identification of adropin as a secreted factor linking dietary macronutrient intake with energy homeostasis and lipid metabolism. Cell Metab. *8*, 468–481.

Lai, K.K., Kolippakkam, D., and Beretta, L. (2008). Comprehensive and quantitative proteome profiling of the mouse liver and plasma. Hepatology *47*, 1043–1051.

Larson-Meyer, D.E., Newcomer, B.R., Ravussin, E., Volaufova, J., Bennett, B., Chalew, S., Cefalu, W.T., and Sothern, M. (2011). Intrahepatic and intramyocellular lipids are determinants of insulin resistance in prepubertal children. Diabetologia *54*, 869–875.

Linder, K., Springer, F., Machann, J., Schick, F., Fritsche, A., Häring, H.U., Blumenstock, G., Ranke, M.B., Stefan, N., Binder, G., and Ehehalt, S. (2014). Relationships of body composition and liver fat content with insulin resistance in obesity-matched adolescents and adults. Obesity (Silver Spring) *22*, 1325–1331.

Mason, R.R., Mokhtar, R., Matzaris, M., Selathurai, A., Kowalski, G.M., Mokbel, N., Meikle, P.J., Bruce, C.R., and Watt, M.J. (2014). PLIN5 deletion remodels intracellular lipid composition and causes insulin resistance in muscle. Mol. Metab. *3*, 652–663.

Mathews, S.T., Singh, G.P., Ranalletta, M., Cintron, V.J., Qiang, X., Goustin, A.S., Jen, K.L., Charron, M.J., Jahnen-Dechent, W., and Grunberger, G. (2002). Improved insulin sensitivity and resistance to weight gain in mice null for the Ahsg gene. Diabetes *51*, 2450–2458.

Mevorach, M., Giacca, A., Aharon, Y., Hawkins, M., Shamoon, H., and Rossetti, L. (1998). Regulation of endogenous glucose production by glucose per se is impaired in type 2 diabetes mellitus. J. Clin. Invest. *102*, 744–753.

Misu, H., Takamura, T., Takayama, H., Hayashi, H., Matsuzawa-Nagata, N., Kurita, S., Ishikura, K., Ando, H., Takeshita, Y., Ota, T., et al. (2010). A liver-derived secretory protein, selenoprotein P, causes insulin resistance. Cell Metab. *12*, 483–495.

Mori, K., Emoto, M., Yokoyama, H., Araki, T., Teramura, M., Koyama, H., Shoji, T., Inaba, M., and Nishizawa, Y. (2006). Association of serum fetuin-A with insulin resistance in type 2 diabetic and nondiabetic subjects. Diabetes Care *29*, 468.

Morton, G.J., Matsen, M.E., Bracy, D.P., Meek, T.H., Nguyen, H.T., Stefanovski, D., Bergman, R.N., Wasserman, D.H., and Schwartz, M.W. (2013). FGF19 action in the brain induces insulin-independent glucose lowering. J. Clin. Invest. *123*, 4799–4808.

Nishida, Y., Higaki, Y., Tokuyama, K., Fujimi, K., Kiyonaga, A., Shindo, M., Sato, Y., and Tanaka, H. (2001). Effect of mild exercise training on glucose effectiveness in healthy men. Diabetes Care *24*, 1008–1013.

Oike, Y., Akao, M., Yasunaga, K., Yamauchi, T., Morisada, T., Ito, Y., Urano, T., Kimura, Y., Kubota, Y., Maekawa, H., et al. (2005). Angiopoietin-related growth factor antagonizes obesity and insulin resistance. Nat. Med. *11*, 400–408.

Pal, D., Dasgupta, S., Kundu, R., Maitra, S., Das, G., Mukhopadhyay, S., Ray, S., Majumdar, S.S., and Bhattacharya, S. (2012). Fetuin-A acts as an endogenous ligand of TLR4 to promote lipid-induced insulin resistance. Nat. Med. *18*, 1279–1285.

Petersen, K.F., Dufour, S., Befroy, D., Lehrke, M., Hendler, R.E., and Shulman, G.I. (2005). Reversal of nonalcoholic hepatic steatosis, hepatic insulin resistance, and hyperglycemia by moderate weight reduction in patients with type 2 diabetes. Diabetes *54*, 603–608.

Samuel, V.T., and Shulman, G.I. (2012). Mechanisms for insulin resistance: common threads and missing links. Cell *148*, 852–871.

Schmid, G.M., Converset, V., Walter, N., Sennitt, M.V., Leung, K.Y., Byers, H., Ward, M., Hochstrasser, D.F., Cawthorne, M.A., and Sanchez, J.C. (2004). Effect of high-fat diet on the expression of proteins in muscle, adipose tissues, and liver of C57BL/6 mice. Proteomics *4*, 2270–2282.

Stefan, N., and Häring, H.U. (2013a). Circulating fetuin-A and free fatty acids interact to predict insulin resistance in humans. Nat. Med. *19*, 394–395.

Stefan, N., and Häring, H.U. (2013b). The role of hepatokines in metabolism. Nat. Rev. Endocrinol. *9*, 144–152.

Stefan, N., Hennige, A.M., Staiger, H., Machann, J., Schick, F., Kröber, S.M., Machicao, F., Fritsche, A., and Häring, H.U. (2006). Alpha2-Heremans-Schmid glycoprotein/fetuin-A is associated with insulin resistance and fat accumulation in the liver in humans. Diabetes Care *29*, 853–857.

Stewart, L.K., Wang, Z., Ribnicky, D., Soileau, J.L., Cefalu, W.T., and Gettys, T.W. (2009). Failure of dietary quercetin to alter the temporal progression of insulin resistance among tissues of C57BL/6J mice during the development of diet-induced obesity. Diabetologia *52*, 514–523.

Strissel, K.J., Stancheva, Z., Miyoshi, H., Perfield, J.W., 2nd, DeFuria, J., Jick, Z., Greenberg, A.S., and Obin, M.S. (2007). Adipocyte death, adipose tissue remodeling, and obesity complications. Diabetes *56*, 2910–2918.

Tonelli, J., Kishore, P., Lee, D.E., and Hawkins, M. (2005). The regulation of glucose effectiveness: how glucose modulates its own production. Curr. Opin. Clin. Nutr. Metab. Care *8*, 450–456.

Toye, A.A., Dumas, M.E., Blancher, C., Rothwell, A.R., Fearnside, J.F., Wilder, S.P., Bihoreau, M.T., Cloarec, O., Azzouzi, I., Young, S., et al. (2007). Subtle metabolic and liver gene transcriptional changes underlie diet-induced fatty liver susceptibility in insulin-resistant mice. Diabetologia *50*, 1867–1879.

Turner, N., Kowalski, G.M., Leslie, S.J., Risis, S., Yang, C., Lee-Young, R.S., Babb, J.R., Meikle, P.J., Lancaster, G.I., Henstridge, D.C., et al. (2013). Distinct patterns of tissue-specific lipid accumulation during the induction of insulin resistance in mice by high-fat feeding. Diabetologia *56*, 1638–1648.

Wicklow, B.A., Wittmeier, K.D., MacIntosh, A.C., Sellers, E.A., Ryner, L., Serrai, H., Dean, H.J., and McGavock, J.M. (2012). Metabolic consequences of hepatic steatosis in overweight and obese adolescents. Diabetes Care *35*, 905–910.

Xu, H., Barnes, G.T., Yang, Q., Tan, G., Yang, D., Chou, C.J., Sole, J., Nichols, A., Ross, J.S., Tartaglia, L.A., and Chen, H. (2003). Chronic inflammation in fat plays a crucial role in the development of obesity-related insulin resistance. J. Clin. Invest. *112*, 1821–1830.

Younossi, Z.M., Baranova, A., Ziegler, K., Del Giacco, L., Schlauch, K., Born, T.L., Elariny, H., Gorreta, F., VanMeter, A., Younoszai, A., et al. (2005). A genomic and proteomic study of the spectrum of nonalcoholic fatty liver disease. Hepatology *42*, 665–674.

Zhang, M., and Schekman, R. (2013). Cell biology. Unconventional secretion, unconventional solutions. Science *340*, 559–561.

Zhang, X., Yang, J., Guo, Y., Ye, H., Yu, C., Xu, C., Xu, L., Wu, S., Sun, W., Wei, H., et al. (2010). Functional proteomic analysis of nonalcoholic fatty liver disease in rat models: enoyl-coenzyme a hydratase down-regulation exacerbates hepatic steatosis. Hepatology *51*, 1190–1199.